Excitation of parasitic waves in forward-wave amplifiers with weak guiding fields

G. S. Nusinovich, C. A. Romero-Talamás, and Y. Han
Institute for Research in Electronics and Applied Physics, University of Maryland, College Park, Maryland 20742-3511, USA
(Received 18 October 2012; revised manuscript received 27 November 2012; published 19 December 2012)

To produce high-power coherent electromagnetic radiation at frequencies from microwaves up to terahertz, the radiation sources should have interaction circuits of large cross sections, i.e., the sources should operate in high-order modes. In such devices, the excitation of higher-order parasitic modes near cutoff where the group velocity is small and, hence, start currents are low can be a serious problem. The problem is especially severe in the sources of coherent, phase-controlled radiation, i.e., the amplifiers or phase-locked oscillators. This problem was studied earlier [Nusinovich, Sinitsyn, and Antonsen, Phys. Rev. E **82**, 046404 (2010)] for the case of electron focusing by strong guiding magnetic fields. For many applications it is desirable to minimize these focusing fields. Therefore in this paper we analyze the problem of excitation of parasitic modes near cutoff in forward-wave amplifiers with weak focusing fields. First, we study the large-signal operation of such a device with a signal wave only. Then, we analyze the self-excitation conditions of parasitic waves near cutoff in the presence of the signal wave. It is shown that the main effect is the suppression of the parasitic wave in large-signal regimes. At the same time, there is a region of device parameters where the presence of signal waves can enhance excitation of parasitic modes. The role of focusing fields in such effects is studied.

DOI: 10.1103/PhysRevE.86.066410 PACS number(s): 52.59.Ye, 41.20.Jb, 84.40.Fe

I. INTRODUCTION

Among various sources of high-power coherent electromagnetic (EM) radiation, the devices based on synchronous interaction between electrons propagating in vacuum and slow EM waves whose phase velocity is close to the electron velocity form an important class (see, e.g., Ref. [1]). The EM radiation in such devices is known as the Cherenkov coherent radiation and (in the case of periodic EM circuits) as the Smith-Purcell radiation. Quite often, the Smith-Purcell radiation is treated as a partial case of the Cherenkov radiation because for the beam-wave interaction in this case the same condition of the synchronism between the electron velocity and the phase velocity of one of the space harmonics should be fulfilled. The most known devices based on this type of radiation are traveling-wave tubes, backward-wave oscillators, and orotrons.

There is a strong interest in developing high-power sources of coherent EM radiation at very high frequencies. Primarily, this interest is motivated by such applications as communication and radar systems where the amplifiers with controlled phase and frequency are required [2,3]. At present, this active development is going on in the *W* band (95 GHz) (see, e.g., [4,5]) and at much higher frequencies, such as 220 GHz [6] and even 650–850 GHz where the power of available sources is, at best, at a multimilliwatt level (see review papers [6,7]). This progress is accompanied not only by the development of powerful two-dimensional (2D) and three–dimensional codes, but also by attempts to develop a simplified general theory which would elucidate some basic features in the operation of such devices.

One of the issues critical for the development of high-power amplifiers driven by electron beams is possible excitation of some parasitic oscillations in these amplifiers. As a rule, the most dangerous parasitic modes are those which can be excited at the ends of the passbands. This statement is illustrated by Fig. 1. As known, such waves excited near cutoff frequencies have low group velocities and, hence, can be strongly coupled to the electron beam. Excitation of parasitic waves near cutoff in forward-wave amplifiers was studied in Ref. [8] where the effect of the signal wave on the excitation conditions of such parasitic waves was analyzed. (A similar study of parasitic excitation far from cutoff was carried out in Ref. [9].) In Ref. [8], an analysis was carried out under the assumption that electrons are guided by strong focusing magnetic fields and, therefore, exhibit a one-dimensional (1D) motion along the device axis.

In practice, however, it is desirable to minimize the weight of the focusing systems, i.e., to operate in low focusing fields. A limiting case of operation in the absence of guiding magnetic fields was realized in the device called the pasotron (an acronym for plasma-assisted slow-wave oscillator) which was developed in both oscillator and amplifier configurations [10–12]. Electron motion in such configurations where, in the absence of guiding fields, electrons can move both axially and transversely was studied in Ref. [13]. Later, the amplifier operation in weak magnetic fields was analyzed in Ref. [14]. Note that transverse motion of electrons in weak focusing fields can also affect the self-excitation of forward-wave amplifiers even in the absence of other modes. This issue was addressed in Ref. [15].

Below, we analyze the excitation of parasitic waves near cutoff in amplifiers where electrons are guided by weak magnetic fields. Our study consists of two stages. First, we characterize the operation of a forward-wave amplifier in weak magnetic field. This part of the study is essentially a continuation of the work described in Ref. [14]. Next, we analyze the self-excitation of parasitic waves in the presence of forward waves and the effect of the signal wave on these excitation conditions. This part can be treated as a generalization of the 1D treatment presented in Ref. [8] on a 2D case. Our paper is organized as follows. Section II contains the formulation of the problem. In Sec. III the results are presented. In Sec. IV we discuss the results obtained, and Sec. V summarizes the study.

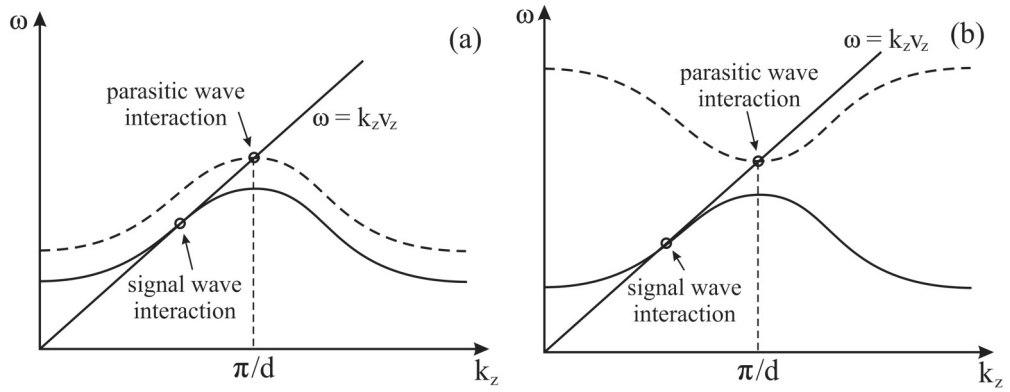

FIG. 1. Dispersion diagrams for the cases when the parasitic mode has the normal (a) and anomalous (b) dispersion.

II. FORMULATION

As described in the Introduction, our study will consist of two stages. The first stage is devoted to the analysis of the operation of a forward-wave amplifier with a weak focusing field. In the course of the second stage we study the self-excitation of parasitic modes near cutoff in the presence of the forward signal wave.

A. Forward-wave amplifier with a weak focusing field

Equations describing the operation of a forward-wave amplifier with a weak focusing magnetic field had been derived in Ref. [14]. Here we will omit details of the derivation, but will just mention that conservation of electron angular momentum allows us to greatly simplify description of electron transverse motion. In notations similar to those used in the theory of traveling-wave tubes [16,17], the self-consistent set of equations can be given as

$$\frac{\partial^2\theta_1}{\partial\varsigma^2} = \hat{I}_0(\rho)\mathrm{Re}\{\alpha_1 e^{i\theta_1}\}, \tag{1}$$

$$\frac{\partial^2\rho}{\partial\varsigma^2} = \hat{I}_1(\rho)\mathrm{Im}\{\alpha_1 e^{i\theta_1}\} + M\frac{\rho_0^4-\rho^4}{\rho^3}, \tag{2}$$

$$\frac{\partial^2\alpha_1}{\partial\varsigma} - i\delta_1\alpha_1 = \frac{1}{\pi}\int_0^{2\pi}\hat{I}_0(\rho)e^{-i\theta_1}d\theta_{10}. \tag{3}$$

Here $\theta_1 = k_{z,s}z - \omega_1 t$ is the phase of electron axial motion with respect to the phase of the synchronous space harmonic of the signal wave. The evolution of this phase in the process of electron motion is described by the nonlinear pendulum equation (1) known not only in the nonlinear theory of the traveling-wave tubes (TWTs) [17], but also in the theory of ubitrons [18] and free electron lasers [19]. In our case, the right-hand side of this equation varies along the axis not only because of the growth of the signal wave amplitude, but also due to changes in the radial location of an electron. The latter changes depend on the electron phase at the entrance θ_{10}. The boundary conditions to Eq. (1) are $\theta_1(\varsigma=0)=\theta_{10}\in[0,2\pi), \partial\theta/\partial\varsigma|_{\varsigma=0}=0$.

Equation (2) describes electron radial motion in the case of the focusing force (characterized by the parameter M defined below) of the same order as the force caused by the radial component of the wave electric field. In the case of strong focusing, the first term in the right-hand side of Eq. (2) can be ignored. Then, this equation is reduced to the beam envelope equation (5.82) of Ref. [20] with a negligible space charge force. Correspondingly, in the case of the beam injection parallel to the device axis, the solution of Eq. (2) will be simply $\rho=\rho_0$. In Eq. (2), we use the variable $\rho = |k_{\perp s}|r_b$, which is the radial coordinate of electrons r_b multiplied by the absolute value of the transverse wave number of the synchronous space harmonic of the wave. The boundary conditions to Eq. (2) are $\rho(\varsigma=0)=\rho_0$, $\partial\rho/\partial\varsigma|_{\varsigma=0}=0$; i.e., we assume at the entrance a thin annular beam of electrons moving along the axis. Equation (3) describes the wave excitation by an electron beam in which the axial electron momentum is much larger than the transverse one, $p_z \gg p_\perp$, and therefore, the role of the transverse interaction between the wave and electrons is not important for the wave amplification. When the wave amplitude is not too large and the interaction length is long enough, the radial displacement of electrons upon the action of the radial electric wave field may lead to the beam interception by the wall even when the radial momentum of electrons is small.

All other parameters in Eqs. (1)–(3) are normalized to the Pierce-like gain parameter C. In our case this parameter for a slow-wave structure of the period d and length $L$is defined by

$$C^3 = \frac{eI_b}{mc^3}\frac{dL^2}{U\beta_{\mathrm{gr}}}\kappa^2 I_0^2(\rho_0). \tag{4}$$

In Eq. (4), I_b is the beam current, U is the energy of a wave of the unit amplitude stored in one period of the structure (corresponding derivation is given elsewhere [21]), β_{gr} is the wave group velocity normalized to the speed of light, $\kappa = |k_{\perp s}|/(\omega_1/c)$ is the absolute value of the imaginary transverse wave number of the synchronous space harmonic of the signal wave normalized to ω_1/c, and $I_0(\rho_0)$ is the zero-order modified Bessel function defining the coupling of the signal wave to an annular electron beam at the entrance to the interaction space. Note that the condition of the Cherenkov synchronism between electrons and a slow wave, $v_{\mathrm{ph}} = \omega/k_z \approx v_{\mathrm{el}}$, allows one to redefine the normalized transverse wave number given above as $\kappa^2 = (k_z c/\omega)^2 - 1 \approx (1/\beta_0)^2 - 1 = 1/\gamma_0^2\beta_0^2$ (here $\gamma_0 = 1/\sqrt{1-\beta_0^2}$ is the Lorentz factor). Hence, the parameters in Eqs. (1)–(3) can be expressed as $\varsigma = C(z/L)$, $\alpha = [(eAL/mc^2)\kappa I_0(\rho_0)]/C^2$, and $M = [(\omega_L L/c\gamma_0\beta_0)^2]/C^2$ (here $\omega_L = eB_0/2mc$ is the electron Larmor frequency

proportional to the guiding magnetic field B_0). Also, in Eq. (3) $\delta_1 = [(\omega_1 - k_{z1}v_{z0})L/v_{z0}]/C$ is the normalized detuning of the Cherenkov synchronism (this detuning is identical to the velocity parameter used by Pierce [16]). In Eqs. (1)–(3) the Bessel functions with a "hat" are the modified Bessel functions (of the zero and first order for the axial and radial components of the wave electric field, respectively) normalized to $I_0(\rho_0)$. The device operation without guiding fields, i.e., Eqs. (1)–(3) with $M = 0$, was analyzed in Ref. [13], while an opposite case of infinitely strong focusing fields when electrons exhibit 1D motion was studied in Ref. [8].

Correspondingly, the interaction efficiency

$$\eta = (\gamma_0 - \langle\gamma(L)\rangle)/(\gamma_0 - 1) \tag{5}$$

[angular brackets in Eq. (5) denote averaging over the entrance phases] can be rewritten in these notations as

$$\eta = (\gamma_0 + 1)\sqrt{\gamma_0^2 - 1}C\hat{\eta}, \tag{6}$$

where the normalized efficiency $\hat{\eta}$ is determined by the solution of Eqs. (1)–(3):

$$\hat{\eta} = \frac{1}{2\pi}\int_0^{2\pi}\left.\frac{\partial\theta_1}{\partial\varsigma}\right|_{\varsigma_{\rm out}} d\theta_{10}. \tag{7}$$

B. Excitation of parasitic waves near cutoff in the presence of forward waves

Below, we consider only the conditions for self-excitation of the parasitic mode, i.e., assume that the amplitude of this mode is small and, hence, the problem can be treated in the small-signal approximation, while the electron motion is already strongly affected by the field of the forward wave operating in the large-signal regime. Then, using the same assumptions as in Ref. [8] and repeating the same steps in the derivation as those described for the case of linear (1D) electron motion there, one can arrive at the condition for the excitation of the parasitic wave near cutoff in the form of Eq. (25) of Ref. [8]:

$$G_2 \geqslant |f_2(\varsigma_{\rm out})|^2 \frac{|E_{1z}(\vec{r}_{b0})|^2}{|E_{2z}(\vec{r}_{b0})|^2}\frac{U_2\omega_1}{U_1\omega_2}\frac{1}{\beta_{\rm gr1}}\left|h_2\frac{d\beta_{\rm gr2}}{dh_2}\right|_{h_{20}}\Bigg|. \tag{8}$$

Here, in the right-hand side the function $f_2(\varsigma)$ describes the axial structure of the parasitic mode whose field is represented as $A_2(t)f_2(\varsigma)$. Also, we have the ratio of the beam coupling parameters (squared modified Bessel functions of the zero order) defined at the entrance to the interaction space, while in Ref. [8] these parameters remained constant along the axis. The last ratio in the right-hand side of Eq. (8), viz., $(1/\beta_{\rm gr1})h_2(d\beta_{\rm gr2}/dh_2|_{h_{20}})$, depends on the type of slow-wave structure and the points where the beam line intersects dispersion curves of the operating and the parasitic waves.

The gain function of the parasitic mode G_2 in the left-hand side of Eq. (8) can be determined (cf. Ref. [8]) as

$$G_2 = \frac{\partial}{\partial\delta_2}\frac{1}{2\pi}\int_0^{2\pi}\left\{\left|\int_0^{\varsigma_{\rm out}} f_2\hat{I}_0\left[\frac{\kappa_2}{\kappa_1}\rho(\varsigma,\theta_{10})\right]e^{i(\delta_2\varsigma+\theta_1)}d\varsigma\right|^2\right\} \times d\theta_{10}. \tag{9}$$

Equation (9) takes into account the changes in the electron coupling to the parasitic wave due to the radial motion. The argument of this modified Bessel function contains the ratio of normalized transverse wave numbers of two waves with different frequencies and different axial wave numbers. However, since both waves obey the condition of the Cherenkov synchronism, their transverse wave numbers are equal and, therefore, this ratio is equal to unity; so below we will simply use $\hat{I}_0[\rho(\varsigma,\theta_{10})]$. Formula (9) defines the derivative of the spectral intensity of the EM force acting upon electrons exhibiting a 2D motion. The important feature of our treatment is the fact that this small-signal gain function of the parasitic mode depends on the electron interaction with the signal forward wave: the electron phase θ_1 and the radial coordinate ρ are defined by Eqs. (1) and (2), respectively.

III. RESULTS

A. Large-signal operation of a forward-wave amplifier with a weak focusing field

Since the small-signal theory of a TWT operating in a weak magnetic field was developed by J. Pierce a long time ago [16], we present here only some results of large-signal calculations. These results can be treated as complementing those given in Ref. [14].

Figure 2(a) shows the wave amplification along the device axis for the case of exact synchronism between the electron

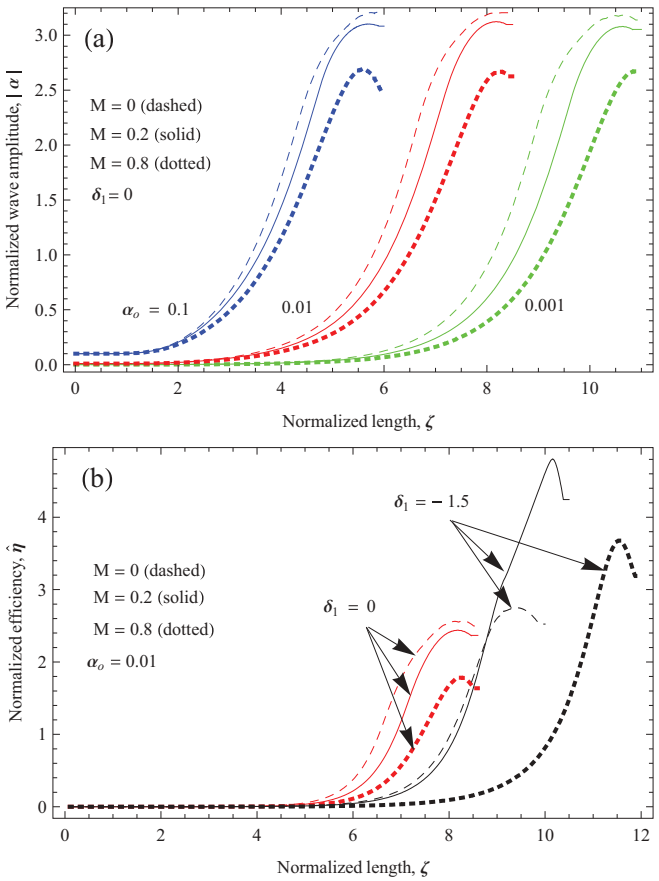

FIG. 2. (Color online) The wave amplitude (a) and the normalized efficiency (b) as the functions of the normalized length.

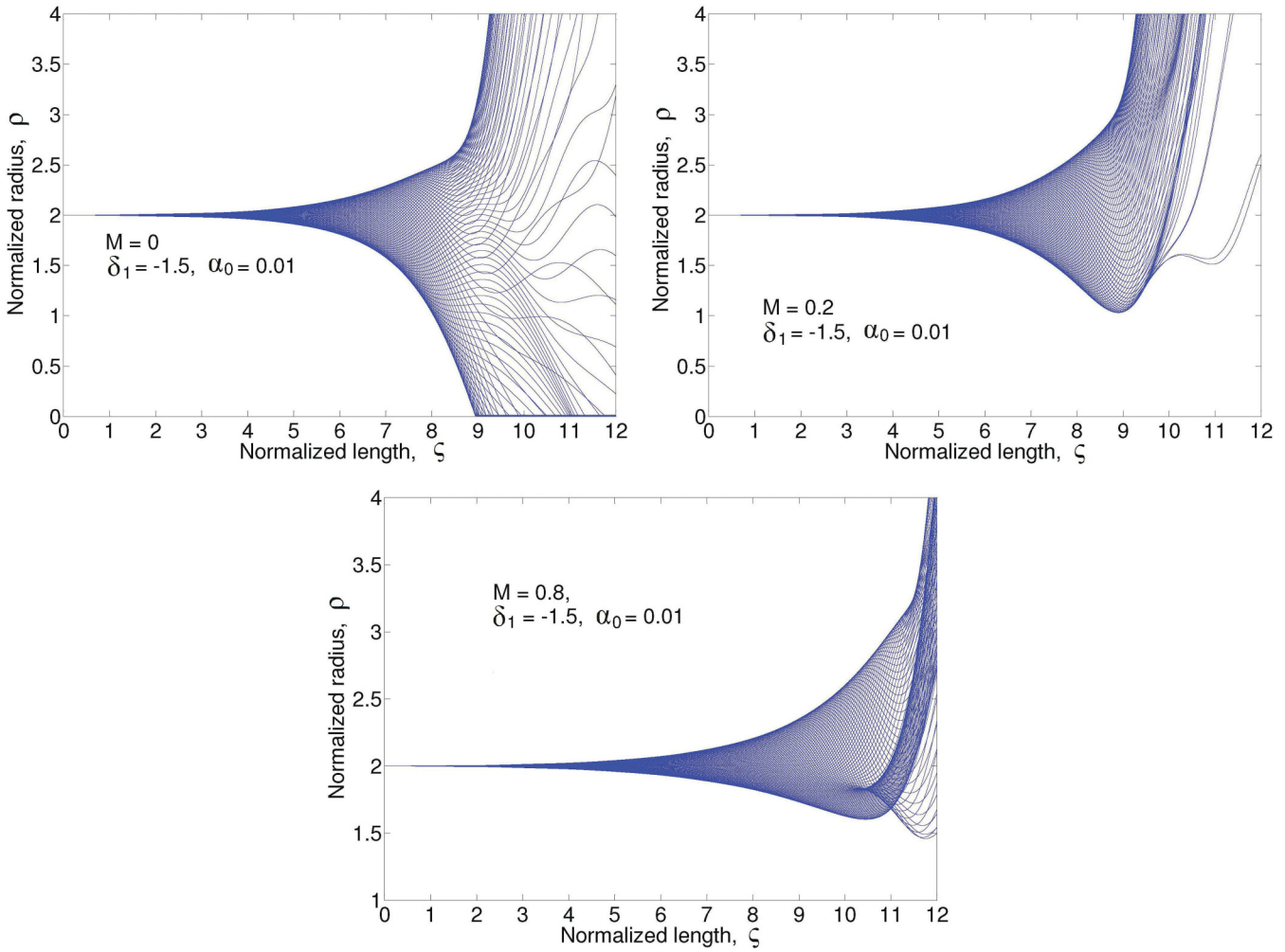

FIG. 3. (Color online) Electron beam propagation at different values of the focusing parameter M.

initial velocity and the signal wave phase velocity ($\delta_1 = 0$) and for different values of the initial amplitude of the signal wave. The dashed, solid, and dotted lines illustrate the cases of the absence of guiding fields ($M = 0$), the presence of a weak focusing field ($M = 0.2$), and the case of strong focusing fields ($M = 0.8$), respectively. As one can see, increasing the focusing field strength decreases the peak value of the wave amplitude in the saturation regime.

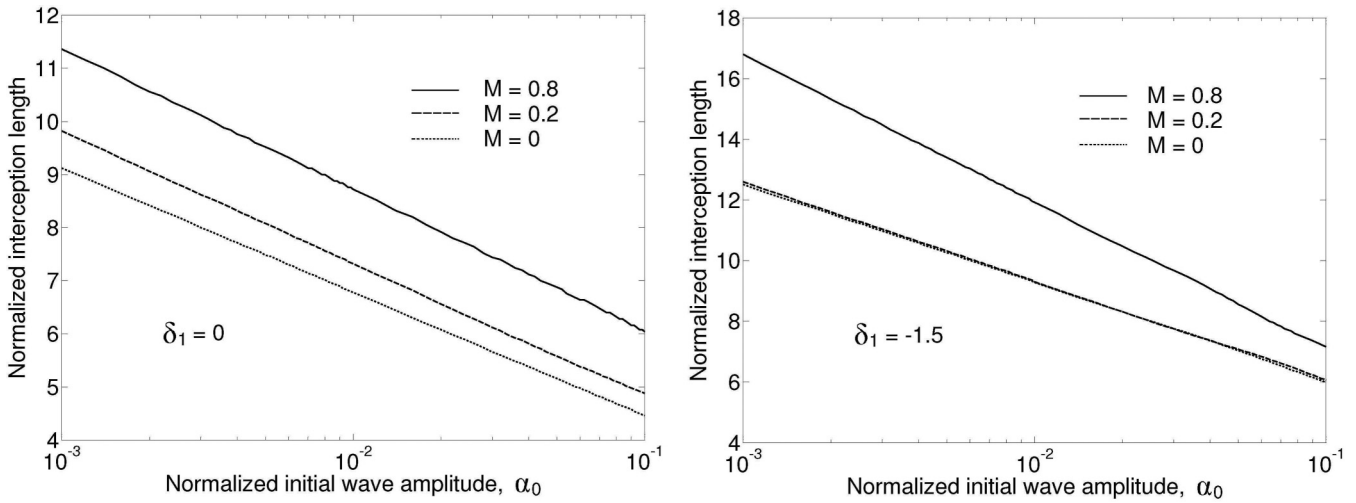

FIG. 4. Beam interception distance as the function of the initial wave amplitude for $\delta_1 = 0$ (a) and $\delta_1 = -1.5$ (b) for several values of the focusing parameter M.

Figure 2(b) shows corresponding dependencies of the normalized efficiency (7) for the cases of exact synchronism ($\delta_1 = 0$) and the optimal detuning ($\delta_1 = -1.5$). In the latter case, the wave grows slower in the linear regime, but then the efficiency becomes higher in the large-signal regime. As one can see, in the case of optimal detunings, the maximum efficiency can be realized in weak focusing fields. The dependence of this efficiency on the parameter M is studied in detail in Ref. [14]. Two limiting cases of strong focusing fields and no focusing fields are studied in Refs. [8] and [13], respectively.

Electron propagation along the device axis in the case of zero focusing fields was studied in Ref. [13]. It was shown that the location of the cross section, where the beam interception by the structure walls starts, strongly depends on the wave detuning δ_1. In the case of exact synchronism ($\delta_1 = 0$), which corresponds to the maximum small-signal gain in the theory of a 1D TWT [16], the interception starts earlier than in the case of high-efficiency operation ($\delta_1 = -1.5$). The electron beam propagation in devices with different values of the focusing parameter M is shown in Fig. 3 for the detuning $\delta_1 = -1.5$. As one can see, at $M = 0$ [Fig. 3(a)] and $M = 0.2$ [Fig. 3(b)] the interception starts practically at the same time. However, at larger values of M [Fig. 3(c)] the interception starts much later.

Corresponding dependencies of the distance where the beam interception starts on the initial amplitude of the signal wave α_0 are shown in Fig. 4 for several values of the focusing parameter M for $\delta_1 = 0$ [Fig. 4(a)] and $\delta_1 = -1.5$ [Fig. 4(b)]. More information about device operation with beam interception can be found in Ref. [14] where the regions of operation with maximum efficiency without beam interception in the plane of parameters "normalized detuning δ_1 versus focusing parameter$M$" were determined.

Figures 5 and 6 below characterize the gain and bandwidth of the device at different values of the focusing magnetic field. Results presented in Fig. 5 show the gain as the function of the initial wave amplitude in the cases $\delta_1 = 0$ [Fig. 5(a)] and $\delta_1 = -1.5$ [Fig. 5(b)] for different values of the focusing parameter$M$. Calculations are done for the normalized length of the interaction space $\varsigma_{\text{out}} = 5$ because, as follows from Fig. 4, with this length one can avoid beam interception even at rather large values of the initial wave amplitude. Note that when the focusing parameter is equal to 0.2 [green, lowest line in Fig. 5(b)], there is a small region of initial amplitudes where the gain increases with the input power. This effect, apparently, has a common nature with the regime of hard self-excitation in oscillators, in which the susceptibility of an electron beam to the electromagnetic field, first, increases with the field intensity and only then saturates. At longer lengths, of course, the gain can be much larger. Results presented in Fig. 5(c) illustrate the fact that the optimal detuning for maximizing the gain depends on the initial wave amplitude. Therefore the detuning $\delta_1 = -0.5$ is close to optimum when the initial amplitude is less than 0.08, but for initial amplitudes larger than 0.09 the optimal value of the detuning is closer to -1.0.

In Fig. 6, the gain is shown as the function of the normalized detuning δ_1 for several values of the focusing parameter M. These results indicate that the value of M has a weak effect on the maximum gain as well as on the bandwidth. Corresponding values of the normalized bandwidth expressed in terms of the range of δ_1 corresponding to the deviation in the gain

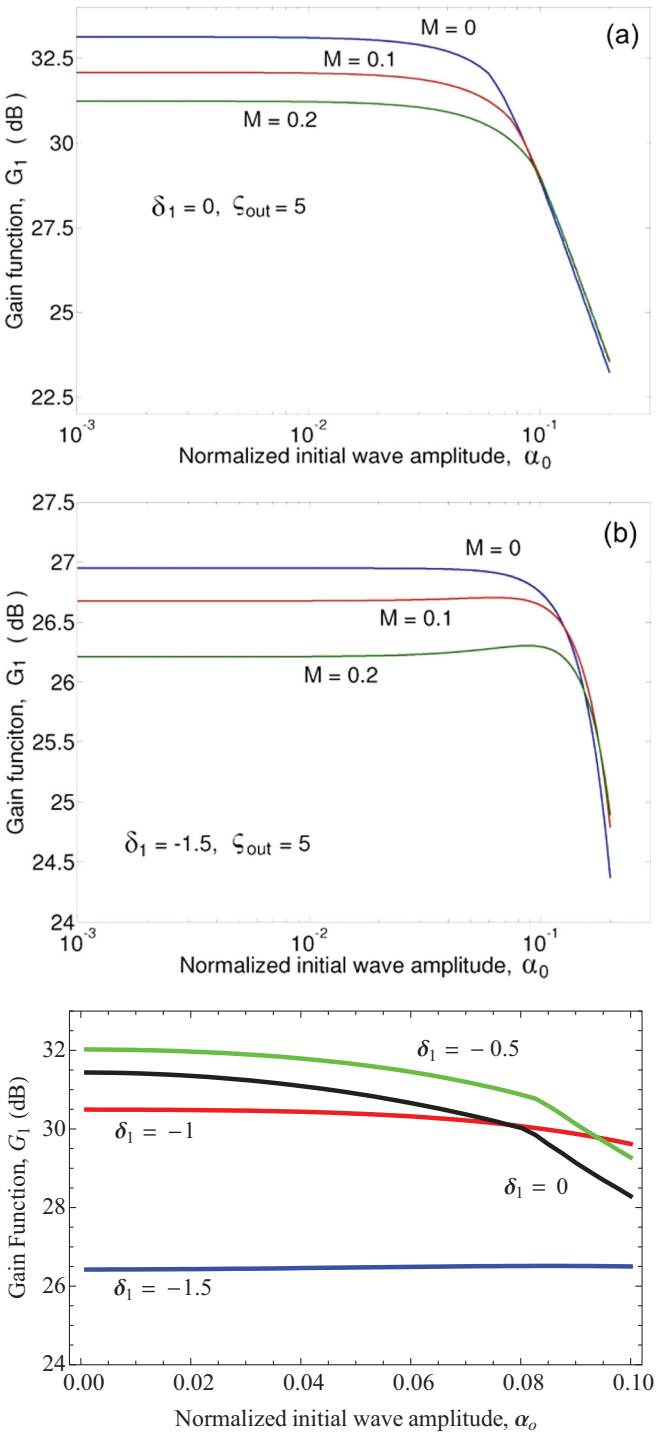

FIG. 5. (Color online) The gain of the signal wave as the function of the initial amplitude of the wave. (c) corresponds to$M = 0.2$.

less than -3 dB of its maximum value are given in Fig. 6. A comparison of Figs. 6(a) and 6(b) reveals the fact that, as the initial wave amplitude increases, the optimal detuning providing the maximum gain shifts towards negative δ_1.

B. Self-excitation of the parasitic mode

We have started our analysis from calculations of the gain function of the parasitic wave in the presence of the signal

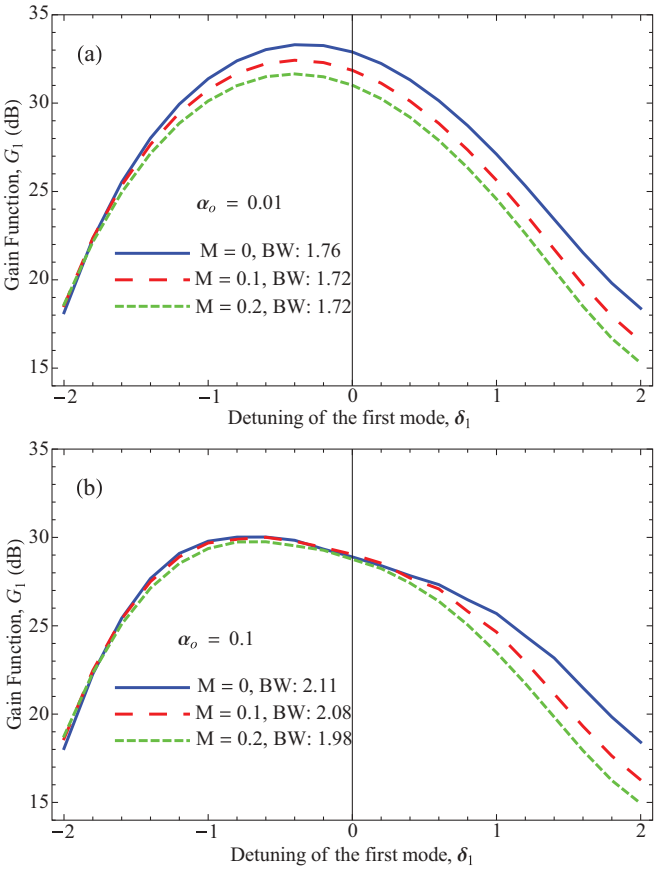

FIG. 6. (Color online) The gain of the signal wave as the function of the detuning δ_1 for the initial wave amplitude of (a) $\alpha_0 = 0.01$ and (b) $\alpha_0 = 0.1$. The bandwidth is defined at -3 dB level of the maximum gain. The normalized interaction length is $\varsigma_{\text{out}} = 5$.

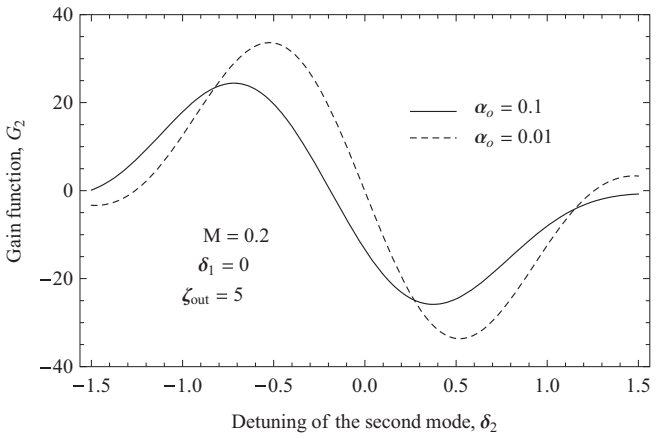

FIG. 7. Gain function of the parasitic mode in the presence of the signal wave.

wave. Calculations were done for the case of a circuit with strong end reflections for the parasitic mode, while the same circuit was assumed above to be well matched for the signal wave (no reflections). It was assumed that the beam line intersects the dispersion curve of the parasitic wave exactly at the π point that allows one to describe the axial structure of the parasitic mode [the function $f(\varsigma)$ in Eqs. (8) and (9)] by $f(\varsigma) = 1$. The effect of a small departure from the π point on the gain function of the parasitic mode was analyzed in Ref. [8]: it leads to reduction of this gain function.

The gain function of the parasitic mode is shown in Fig. 7 for the zero detuning of the signal wave and two values of the initial amplitude of the signal wave: $\alpha_{10} = 0.01$ when the signal wave operates in the small-signal regime and $\alpha_{10} = 0.1$ when the device operates in the regime of saturation. In the case of nonzero detunings the effect of suppression of the parasitic mode is very similar; the curve calculated for the detuning equal to -1.0 and initial wave amplitude equal to 0.1 is practically indistinguishable from the solid line shown in Fig. 7.

Resulting plots showing the region of self-excitation of the parasitic mode in the plane of detunings of the Cherenkov synchronism for two waves (δ_1 and δ_2) are given in the panels in Fig. 8; these panels correspond to different values of the focusing parameter M ($M = 0, M = 0.1$, and $M = 20$). Upper panels correspond to the condition $G_2 \geqslant 1$; lower panels correspond to the case when some methods for selective suppression of the parasitic mode are used and therefore this mode for being excited should have a much larger gain function $G_2 \geqslant 20$. Different curves in these panels correspond to different values of the input wave amplitude. When the initial amplitude of the signal wave is small ($\alpha_0 = 0.01$), the region of parasitic self-excitation lies between two vertical black lines. The fact that these lines are practically vertical indicates that the presence of a small amplitude signal wave whose amplification depends on the detuning δ_1 has no effect on the self-excitation conditions of parasitic wave—they depend on the detuning δ_2 only. However, when $\alpha_0 = 0.1$ (red, dash-dotted lines) or $\alpha_0 = 0.2$ (green, dashed lines), the region of self-excitation is deformed under the action of the signal wave. When, in order to excite the parasitic wave, its gain function should exceed 1 (upper row), the excitation region becomes smaller in the region of detunings δ_2 close to zero (right side of all figures in the upper row), but expands in the range of δ_2 between -1.5 and -1.2 (left side of those figures). This deformation agrees with the dependence of the gain function of the parasitic mode shown in Fig. 7: the main peak of this function located between δ_2 equal 0 and -1.0 becomes smaller due to suppression by the signal wave. At the same time, the effect of the signal wave makes this gain function a little larger in the range of negative detunings δ_2 between -1.0 and -1.5. (The latter effect is known as the nonlinear excitation [22] or cross-excitation instability [23,24].) Note that, as follows from the comparison of Fig. 8(e), which is the case of $G_2 = 1$ and $M = 20$, with Fig. 5(a) of Ref. [8], where the case of $G_2 = 1$ is shown for infinitely strong focusing, the regions of excitation of the parasitic wave are almost identical. Hence, the focusing fields which correspond to this value of M are sufficient for realizing the same suppression of parasitic modes as in infinitely strong focusing fields. Recall that, as shown in Fig. 4, at this value of the focusing parameter, the beam interception by the walls starts much later than at small values of M.

In an amplifier where some mode selective methods are used, the region of self-excitation of the parasitic mode (a lower row in Fig. 8) is even more sensitive to the effect of the signal wave. As shown in Fig. 8, in the regime of deep saturation ($\alpha_{10} = 0.2$—green, dashed lines) the self-excitation of the

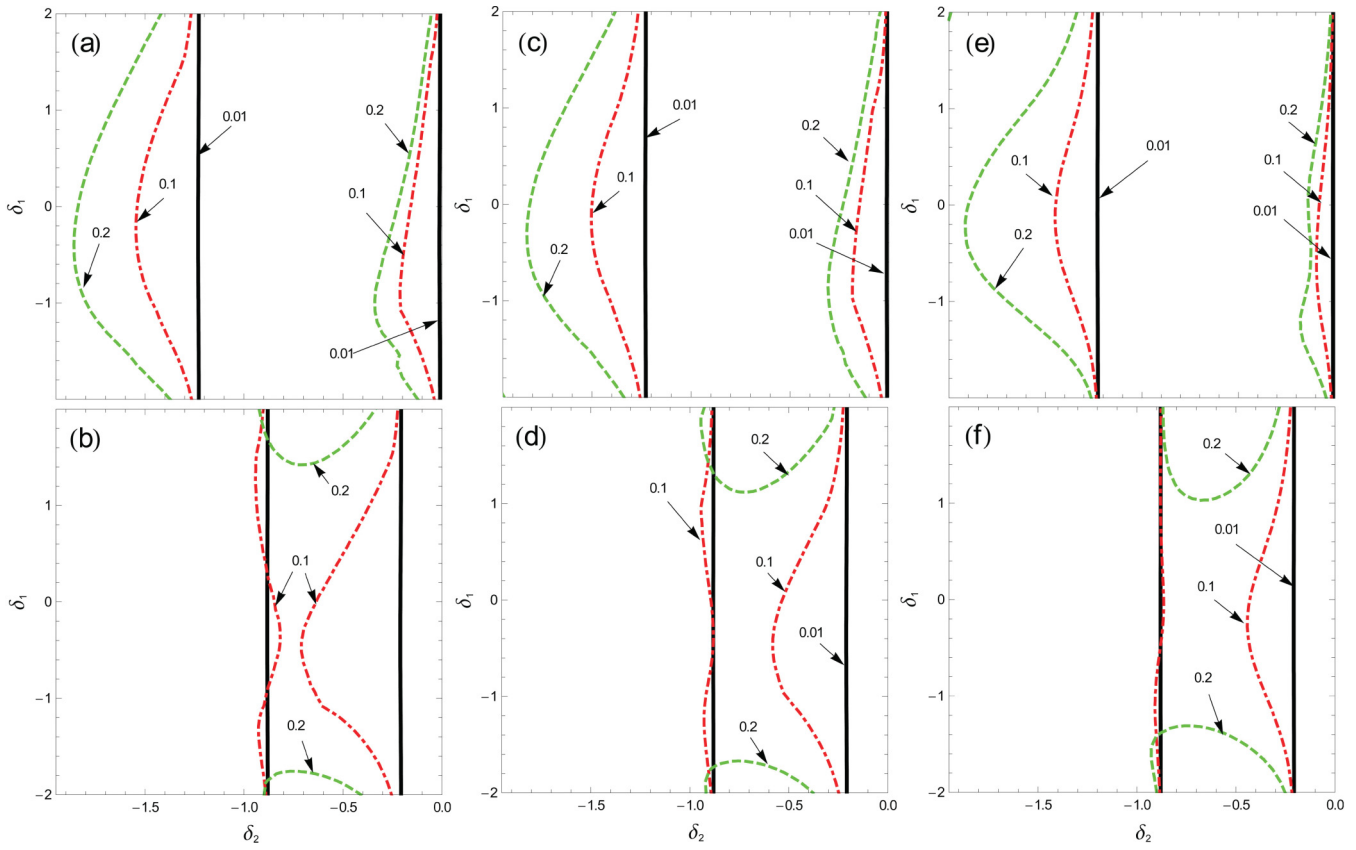

FIG. 8. (Color online) Contours of self-excitation of the parasitic mode in the presence of the signal wave for $M = 0$ [panels (a) and (b)], $M = 0.1$ [panels (c) and (d)], and $M = 20$ [panels (e) and (f)]. The normalized interaction length is $\varsigma_{\text{out}} = 5$. The top panels correspond to $G_2 = 1$, and the bottom panels to $G_2 = 20$. Black (solid), dash-dotted (red), and dashed (green) lines correspond to initial values of the signal wave amplitude α_0 equal to 0.01, 0.1, and 0.2, respectively.

parasitic mode is impossible in a wide range of the detunings δ_1: from -1.4 to 1.2 in the absence of the focusing field [Fig. 8(b)]; from -1.3 to 1.1 in the case of moderate focusing field [Fig. 8(d)]; and from -1.2 to about 1.0 in very strong focusing fields [Fig. 8(f)]. At lower signal wave amplitudes ($\alpha_{10} = 0.1$—red, dash-dotted lines) the region of parasitic self-excitation shrinks as the signal amplitude increases, but it does not disappear completely. A comparison of results shown in Figs. 8(b), 8(d), and 8(f) reveals that the effect of suppression is the strongest in the absence of focusing fields when electrons exhibit the motion in both the axial and transverse directions.

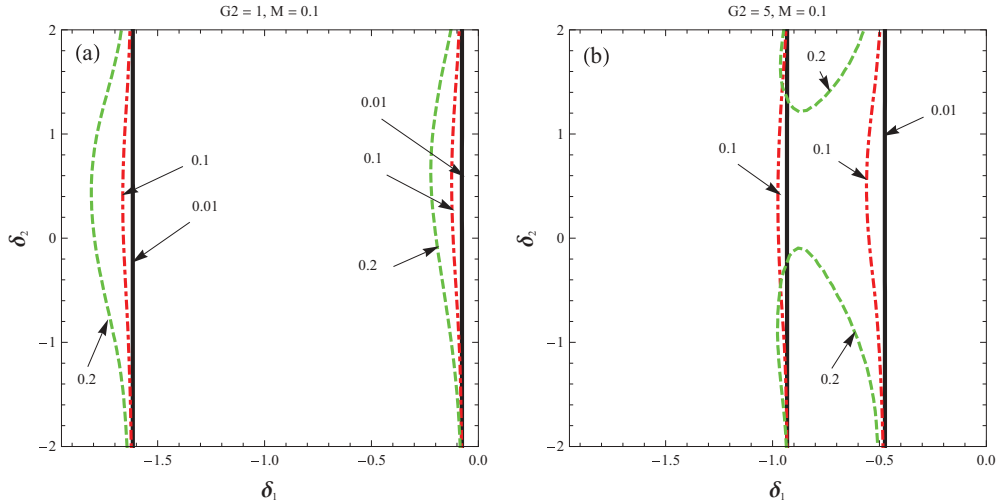

FIG. 9. (Color online) Contours of self-excitation of the parasitic mode shifted of the π point in the presence of the signal wave for $M = 0.1$. (a) and (b) correspond to $G_2 = 1$ and $G_2 = 5$, respectively. Black (solid), dash-dotted (red), and dashed (green) lines correspond to initial values of the signal wave amplitude α_0 equal to 0.01, 0.1, and 0.2, respectively. The normalized interaction length is $\varsigma_{\text{out}} = 5$.

The departure from excitation at the π point decreases the gain function of the parasitic mode. As discussed in Ref. [8], the parasitic mode in this case is formed by two waves of the same frequency, but with slightly different axial wave numbers $k_z = \pi \pm \Delta k_z$. When such waves have large reflections from the ends of a slow-wave structure, they form a standing-wave pattern. Hence, the axial structure of this parasitic mode can be described [8] by the function $f(\varsigma) = (1/2)(1 + \cos\Delta\varsigma)$. Here the detuning Δ is proportional to the departure of the axial wave number from the π point: $\Delta\varsigma = 2(\Delta k_z)z$. The effect of suppression of this mode by the operating wave is illustrated by Fig. 9 given for the case of $\Delta = \pi/\varsigma_{\text{out}}$. [Note that results shown in Fig. 4 of Ref. [8] correspond to $\Delta = \pi/2\varsigma_{\text{out}}$ and $\Delta = \pi/\varsigma_{\text{out}}$.] In Fig. 9, contours of self-excitation of the parasitic mode are shown for the cases of $G_2 = 1$ (a) and $G_2 = 5$ (b) in the same plane of detunings as in Fig. 8. Again, if, for example, for being excited the parasitic mode should have the gain function larger than 5 [Fig. 9(b)], such mode can be excited when the signal wave amplitude is small, but the excitation will be suppressed by a signal wave of large amplitude ($\alpha_{10} = 0.2$) in a certain range of the signal wave detunings δ_1 (between -0.1 and 1.2).

IV. DISCUSSION

Let us consider an example showing what follows from the results of our treatment done in normalized parameters for a sample device. First of all, let us estimate the magnetic field which corresponds to $M = 0.1$, which is the range of focusing parameter values yielding the maximum efficiency [14]. Assume that an X-band device (10 GHz frequency) is driven by a 30 kV, 5 A electron beam, a thin annular beam at the entrance has the radius $\rho_0 = 2$, a periodic slow-wave structure (SWS) consists of 30 periods, the group velocity of the signal wave is $\beta_{\text{gr}} = 0.5$, and the ratio d^3/U in Eq. (4), which relates the energy of a wave of unit amplitude stored in one period of the SWS to this period cubic, is on the order of unity. Then, Eq. (4) yields $C = 2.83$ which corresponds to the gain parameter adopted in Ref. [14] equal to $C_{(14)} = 0.175$. Here these two parameters are related as $C = 2\pi(L/\lambda)C_{(14)}$, and the circuit length expressed in wavelengths relates to the same length expressed in periods of a SWS as $L/\lambda = (\beta_0/4)(L/d)$ (electron velocity normalized to the speed of light for a given voltage is equal to 0.3426). Then, using the definition of the focusing parameter M given after Eq. (4) one can readily find that the value $M = 0.1$ corresponds to the magnetic field close to 144 G. (A similar estimate done in Ref. [14] for a 1.3 GHz plasma-assisted slow-wave oscillator yielded 45 G for $M = 0.2$; this difference can be attributed, in part, to the difference in operating frequencies.) Clearly, such focusing fields can be provided by permanent magnets.

Another comment should be made regarding the departure of the parasitic mode from the dangerous π point. Results presented in Ref. [8] show that the gain function of the parasitic mode is very sensitive to the departure from the π point. To realize this departure either a SWS should be redesigned or the operating voltage should be slightly varied.

V. SUMMARY

The theory describing self-excitation of parasitic modes near cutoff in forward-wave amplifiers operating in weak focusing fields is presented. This theory allows one to analyze the effect of the signal wave on self-excitation conditions of the most dangerous parasitic modes near cutoff. Special emphasis is made on the transverse motion of electrons in weak focusing fields and corresponding limitations on the interaction length in small- and large-signal regimes. It is shown that operation of such amplifiers in large-signal regimes can be more stable than in small-signal regimes due to suppression of parasitic modes by signal waves. It is also shown that even a weak focusing can lead to significant enhancement of the efficiency, while for avoiding the beam interception by the circuit walls a stronger focusing is needed.

ACKNOWLEDGMENTS

This work was supported by the US Air Force Office of Scientific Research and by the Naval Research Laboratory.

[1] L. Schachter, *Beam-Wave Interaction in Periodic and Quasi-Periodic Structures* (Springer, Berlin, 1996).
[2] J. X. Qiu, B. Levush, J. Pasour, A. Katz, C. M. Armstrong, D. R. Whaley, J. Tucek, K. Kreischer, and D. Gallagher, IEEE Microw. Mag. 39 (2009).
[3] W. D. Palmer, Plenary paper at the 13th IVEC and 9th IVESC, Monterey, CA, 2012.
[4] A. Theiss, C. J. Meadows, R. Freeman, R. B. True, J. M. Martin, and K. L. Montgonery, IEEE Trans. Plasma Sci. **38**, 1239 (2010).
[5] W. Gerum, G. Lippert, P. Malzahn, and K. Schneider, IEEE Trans. Electron Devices **48**, 72 (2001).
[6] J. C. Tucek, M. A. Basten, D. A. Gallagher, and K. Kreischer, 13th IVEC and 9th IVESC, Monterey, CA, 2012, paper 26.6, p. 553.
[7] J. H. Booske, R. J. Dobbs, C. D. Joye, C. L. Kory, G. R. Neil, G.-S. Park, J. Park, and R. J. Temkin, IEEE Trans. THz Science and Technol. **1**, 54 (2011).
[8] G. Nusinovich, O. Sinitsyn, and T. Antonsen, Phys. Rev. E **82**, 046404 (2010).
[9] G. Nusinovich, M. Walter, and J. Zhao, Phys. Rev. E **58**, 6594 (1998).
[10] D. Goebel, J. M. Butler, R. W. Schumacher, J. Santoru, and R. L. Eisenhart, IEEE Trans. Plasma Sci. **22**, 547 (1994).
[11] D. M. Goebel, E. S. Ponti, J. R. Feicht, and R. M. Watkins, in Proceedings of Intense Microwave Pulses IV, Denver, CO, 1996 (unpublished), Vol. 2843, p. 69.
[12] A. G. Shkvarunets, Y. Carmel, G. S. Nusinovich, T. M. Abu-elfadl, J. Rodgers, T. M. Antonsen, Jr., V. L. Granatstein, and D. M. Goebel, Phys. Plasmas **9**, 4114 (2002).
[13] G. S. Nusinovich and Yu. P. Bliokh, Phys. Rev. E **62**, 2657 (2000).
[14] T. M. Abu-elfadl, G. S. Nusinovich, A. G. Shkvarunets, Y. Carmel, T. M. Antonsen, Jr., and D. Goebel, Phys. Rev. E **63**, 066501 (2001).

[15] E. M. Ilyina, Yu. F. Kontorin, and S. P. Morev, J. Commun. Technol. Electron. **49**, 937 (2004).
[16] J. R. Pierce, *Traveling-Wave Tubes* (Van Nostrand, Toronto, 1950), Ch. 13.
[17] L. A. Weinstein, Radiotekh. Elektron. (Moscow) **2**, 319 (1957); **2**, 331 (1957).
[18] R. M. Phillips, IRE Trans. Electron Devices **7**, 231 (1960).
[19] J. M. Madey, Nuovo Cimento Soc. Ital. Fis., B **50**, 64 (1978).
[20] M. Reiser, *Theory and Design of Charged Particle Beams* (Wiley-Interscience, New York, 1994), p. 331.
[21] S. M. Miller, T. M. Antonsen, Jr., B. Levush, A. Bromborsky, D. K. Abe, and Y. Carmel, Phys. Plasmas **1**, 730 (1994).
[22] G. S. Nusinovich, Int. J. Electron. **51**, 457 (1981).
[23] B. Levush, T. M. Antonsen, Jr., A. Bromborsky, W. R. Lou, and Y. Carmel, IEEE Trans. Plasma Sci. **20**, 263 (1992).
[24] C. Grabowski, E. Schamiloglu, C. T. Abdallah, and F. Hegeler, Phys. Plasmas **5**, 3490 (1998).